NASA CONTRACTOR REPORT
NASA CR - 134641

CYCLIC FATIGUE ANALYSIS OF ROCKET THRUST CHAMBERS: VOLUME II — ATTITUDE CONTROL THRUSTER HIGH CYCLE FATIGUE

by

Roy W. Miller

Atkins & Merrill Inc.

Ashland, Mass.

June 1974

Prepared for

NATIONAL AERONAUTICS AND SPACE ADMINISTRATION
Lewis Research Center
Cleveland, Ohio

Contract NAS 3-17807
H.G. Price, Project Manager

CONTENTS

PREFACE

A previous report, Reference 1, prepared under this contract, described a computer program, designated RETSCP, for the analysis of rocket engine thrust chambers with cyclic plasticity. That report included a complete description of the program logic, together with a users manual. It is the purpose of this report to illustrate the detailed application of the RETSCP program. Volume I describes the analysis of a regeneratively cooled OFHC copper combustion chamber. Operating conditions are such that plastic strains dominate and fatigue life is in the low cycle regime. Volume II describes the analysis of an attitude control thrust chamber. Operating conditions for that engine are such that the material behavior is elastic, or on the threshold of the elasto-plastic regime; thus, the fatigue life is in the high cycle regime.

SUMMARY

A finite element stress analysis was performed for the film cooled throat section of an attitude control thruster. The analysis employed the RETSCP finite element computer program (NASA CR-134640). The analysis included thermal and pressure loads, and the effects of temperature dependent material properties, to determine the strain range corresponding to the thruster operating cycle. The configuration and operating conditions considered, correspond to a flightweight integrated thruster assembly which was thrust pulse tested at the NASA Lewis Research Center. The computed strain range was used in conjunction with Haynes 188 Universal Slopes minimum life data to predict throat section fatigue life. The computed number of cycles to failure was greater than the number of pulses to which the thruster was experimentally subjected without failure.

INTRODUCTION

As part of the NASA goal to use all cryogenic fueled engines for the reusable Space Shuttle, the necessary technology for reliable attitude control thrusters must be developed. These thrusters are unique in that the life requirements are quite demanding. These 1500 pound (6672 N) thrust engines, using low temperature oxygen and low temperature hydrogen gases, must be capable of firing (pulsing) a minimum of 500 times per mission for 100 missions. As part of this technology effort it becomes imperative that an analytical design procedure be formulated to insure that the fatigue life goal is met under thermal and pressure cycling.

Combustion chambers can be designed to operate at suitable temperature levels by employing film cooling. The thermal analysis of cooled combustion chambers follows established methodology. Empirical data is available for estimating convection heat transfer. The temperature distribution within the structure is then computed using one of many available finite difference computer codes for transient or steady state heat conduction in two or three dimensions.

The state of stress in film cooled rocket chambers varies in three dimensions. The situation is further complicated by the dependence of material properties on temperature. It is the range of strain, through which a given chamber is cycled, that determines fatigue life.

In order to gain experimental data for such attitude control thruster configurations, accelerated testing is attractive. In this manner, fatigue testing is carried out at conditions which are more severe than the normal operating conditions. The resulting stress field may be elastic or may be elasto-plastic.

In this report, a method is described for estimating the fatigue life of attitude control thrusters under normal and accelerated loading conditions. The method itself, has capabilities which exceed the current thruster application. A discussion of possible extensions of the method is given in the Concluding Remarks.

The objective of Volume II of this report is to illustrate in detail the use of the RETSCP finite element computer program for engine configurations where elastic strains dominate; that is, high cycle fatigue. The combustion chamber configuration, operating conditions, and test results are described in sufficient detail to conduct the strain analysis and compare results. These conditions correspond to an engine which was fatigue tested at the NASA Lewis Research Center. The strain analysis is presented in such a manner that the work could be extended to other configurations and operating conditions. The fatigue life analysis section describes the predictive method employed; and, also indicates methods which could be applied for further studies.

ATTITUDE CONTROL THRUSTER CONFIGURATION

The attitude control thruster configuration to be analyzed is shown in Figure 1 from Reference 1. The thruster consists of four major components; namely, injector, thrust chamber, propellant valves, and igniter assembly. These components are integrated to provide a lightweight, compact, high performance thruster, which meets the engine operating conditions and the engine design requirements as shown in Table I and II respectively. The thruster pulse life design requirement is based on 1000 pulses per mission with 100 missions per year and a design safety factor of 5 for a total design pulse life of 500,000 pulses.

Although all attitude control thruster components must be capable of meeting the above requirements; the combustion thrust chamber, which is exposed to a thermal and pressure pulsing environment, deserves the most consideration from the standpoint of fatigue. The combustion thrust chamber is comprised of injector, chamber, throat section, nozzle, torus, liner and flanges which are welded together to form an integral unit.

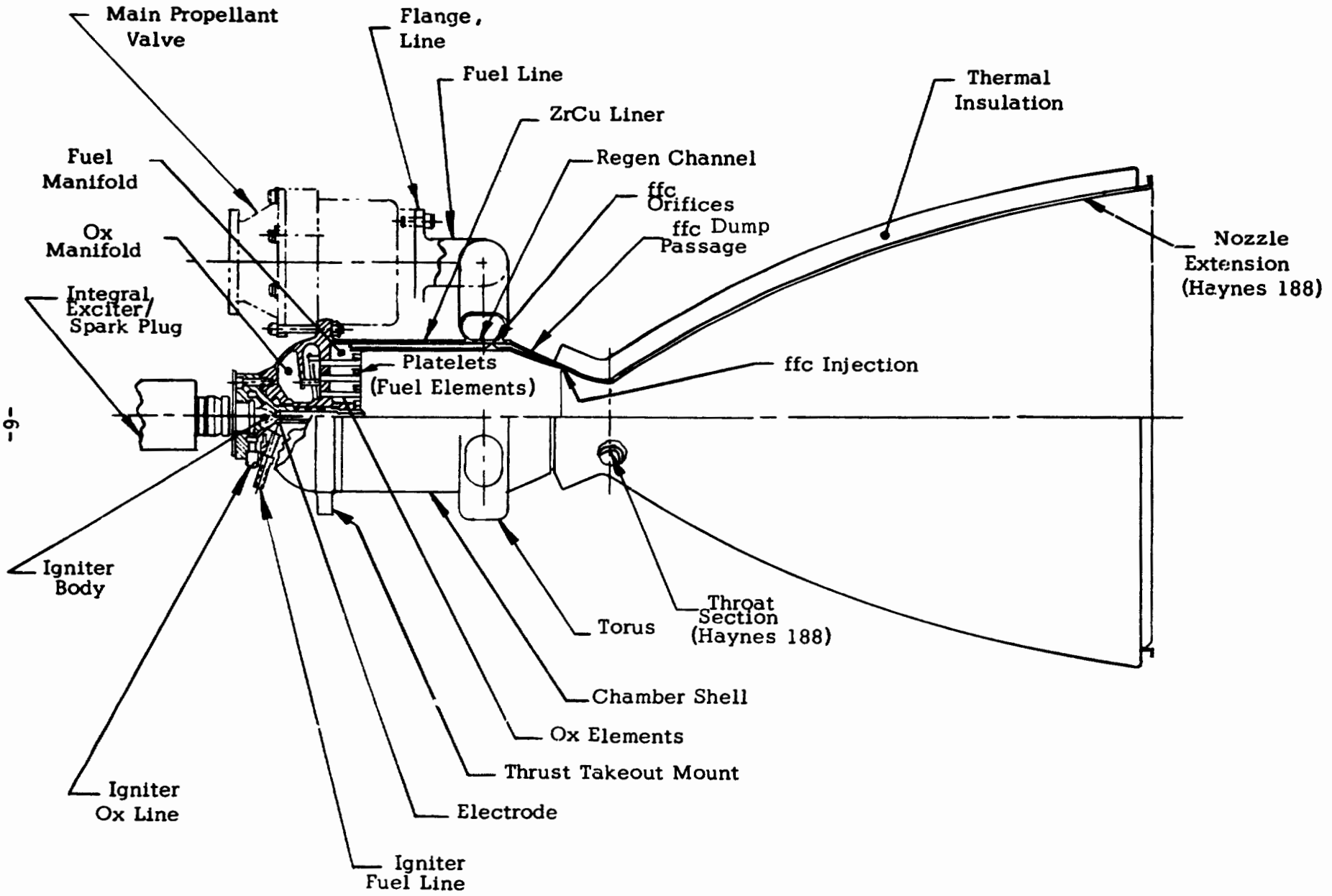

Figure 1. Integrated thruster assembly.

TABLE I
ENGINE OPERATING CONDITIONS
(Nominal Design Values)

Thrust	1500 lb (6672 N)
Chamber Pressure	300 psia (207×10^4 N/m^2)
Mixture Ratio	4.0
Nozzle Expansion Ratio	40.1
Propellant Inlet Temperature:	
Hydrogen	250°R (139°K)
Oxygen	375°R (208°K)
Propellant Inlet Pressure (to Valve):	
Hydrogen	400 psia (276×10^4 N/m^2)
Oxygen	400 psia (276×10^4 N/m^2)
Specific Impulse:	
Steady State	435 lb_f-sec/lb_m (4266 N-sec/kg)
Pulsing Average	400 lb_f-sec/lb_m (3923 N-sec/kg)

TABLE II

ENGINE DESIGN REQUIREMENTS

Fuel:	Gaseous hydrogen derived from the vaporization of liquid hydrogen.
Oxidizer:	Gaseous oxygen derived from the vaporization of liquid oxygen.
Installation:	Buried within vehicle mold line.
Maximum External Temperature:	500°F (260° C)
Total Life Capability:	Estimated 2500 minutes.
Total Number of Firings:	Estimated 500,000 pulses, plus 25,000 deep thermal cycles (full temperature range on each component).
Maximum Single Firing Duration:	500 sec.
Compatibility:	Compatible with propellants, test fluids, cleaning fluids and environmental contaminants for ten-year life requirement.
Reusability:	To be reusable with minimum servicing and refurbishment.
Service and Maintainability:	Design for ease of service and maintenance when required.
Minimum Impulse Bit (goal):	50 lb-sec (222 N-sec)
Response:	50 millisec (time from electrical signal to 90% thrust).
Reentry Heating (goals):	30 minutes exposure per mission to the following temperatures: At nozzle exit plane: 1800°F (982° C) At chamber throat: 1200°F (649° C)
Nozzle Scarfing Capability:	Nozzle skirt shall be easily scarfed beyond an expansion ratio of 25:1.
Weight Goal for Complete Thruster Assembly Less Valves:	15 lb (6804 g)

The injector is a 72 element "premix I" F-O-F triplet design. The face of the injector is made from platelets that contain a fuel [illegible] cooling circuit, the mixing cups, and the 144 "I" shaped fuel passages which discharge approximately 180° apart at right angles to the oxidizer flow (oxidizer flows normal to the face through 72 tubes; fuel flows parallel to the face impinging two fuel elements on each oxidizer element). The hydrogen flow into the injector comes from the outlet of the chamber regenerative passages.

The thrust chamber incorporates a composite cooling system. The major portion of the combustion chamber is regeneratively cooled (80 passages) with fuel. The convergent nozzle contains 160 orificed passages which direct 21% of the fuel flow to a station 1.50 in. (3.81 cm) upstream of the throat where it is introduced as a film coolant. The throat and entire divergent nozzle are of spun Haynes 188 material and operate at the adiabatic wall temperature. The gas-side wall material in the cooled area forward of the fuel film coolant injection station is zirconium copper alloy which contains rectangular cross-section coolant passages. These are closed out by a 22-13-5 stainless steel shell which is brazed to the copper liner. The stainless steel shell is joined to the injector and adiabatic wall nozzle by welding. The composite cooling system results in the fuel inlet manifold (which is also made from 22-13-5 material) being located at the entrance to the convergent nozzle.

The following analysis was conducted specifically at the film cooled throat section. The throat section has 1.92 inch (4.88 cm) inside diameter with 0.030 inch (0.076 cm) wall thickness, and is fabricated from Haynes Alloy No. 188, References 2 and 3.

The engine was pulse tested at the NASA Lewis Research Center. Tests were conducted at 330 psi ($228 \times 10^4 N/m^2$) chamber pressure and the engine developed 1100 pounds (4893 N) thrust. Total pulse time was 0.15 seconds of which approximately 0.10 seconds was operation at full chamber pressure. The outer wall temperature at the nozzle throat was measured, and found to vary from 1040°F (560°C) during engine firing, to 960°F (516° C) during engine-off; once the uniform engine pulse train had been established. It was estimated that the temperature difference (ΔT) across the wall was $\pm$ 180° F ($\pm$100° C). Obviously the inner wall is hotter ($+ \Delta T$) during engine firing. Since the coolant continues to flow after shutdown, the inner wall is cooler ($- \Delta T$) during engine-off. These conditions are represented schematically in Figure 2.

The attitude control thruster was subjected to 50,825 pulses of the above type.

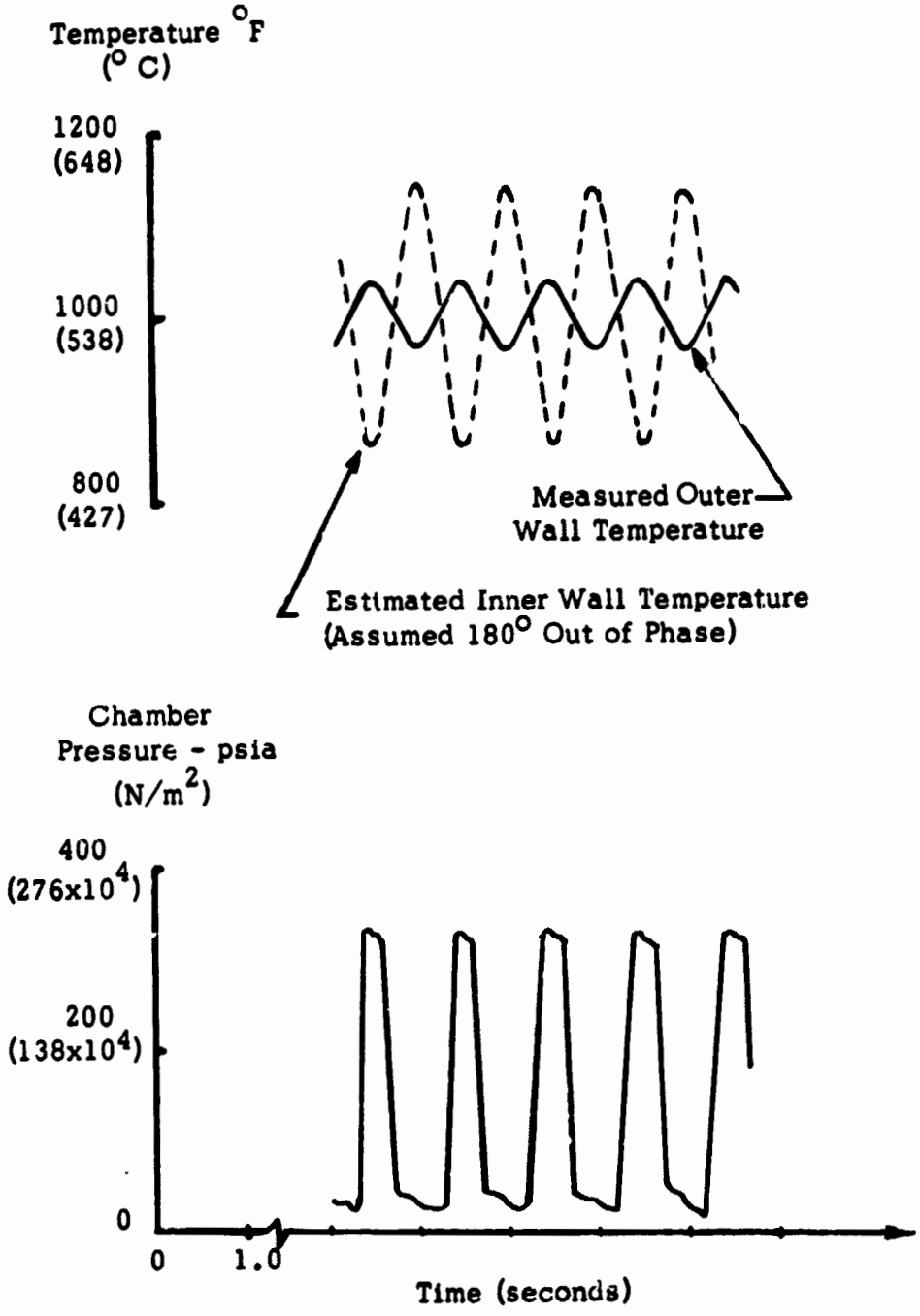

Figure 2. Attitude control thruster test conditions.

STRUCTURAL ANALYSIS

The structural analysis was performed using the RETSCP finite element computer program described in Reference 4. It is well known that fatigue life depends on the cyclic strain range magnitude through which the component is cycled, Reference 5 and 6. Thus, the objective here is to predict the stress-strain cycle for the attitude control thruster throat station.

The RETSCP program used the 12-element model of the throat section shown in Figure 3. Each element has thickness 0.005 inch (0.013 cm) in the z-direction. The model considered is a one degree wedge sector; thus, the section taken is one of 360 symmetric sections. A twelve element model was selected to adequately represent the structure. Smaller elements were provided near the inner wall, where plastic behavior is most likely to occur.

Boundary conditions in the RETSCP program are in the form of prescribed nodal point forces or nodal point displacements. The symmetry of the 12-element model was previously noted. The corresponding boundary condition is zero displacement of boundary points normal to the symmetry plane, and free movement of nodal points in the radial direction. This condition is indicated by the roller notation in Figure 3. The symmetry condition along the 1^{o} surface is accommodated by a coordinate transformation within the RETSCP program.

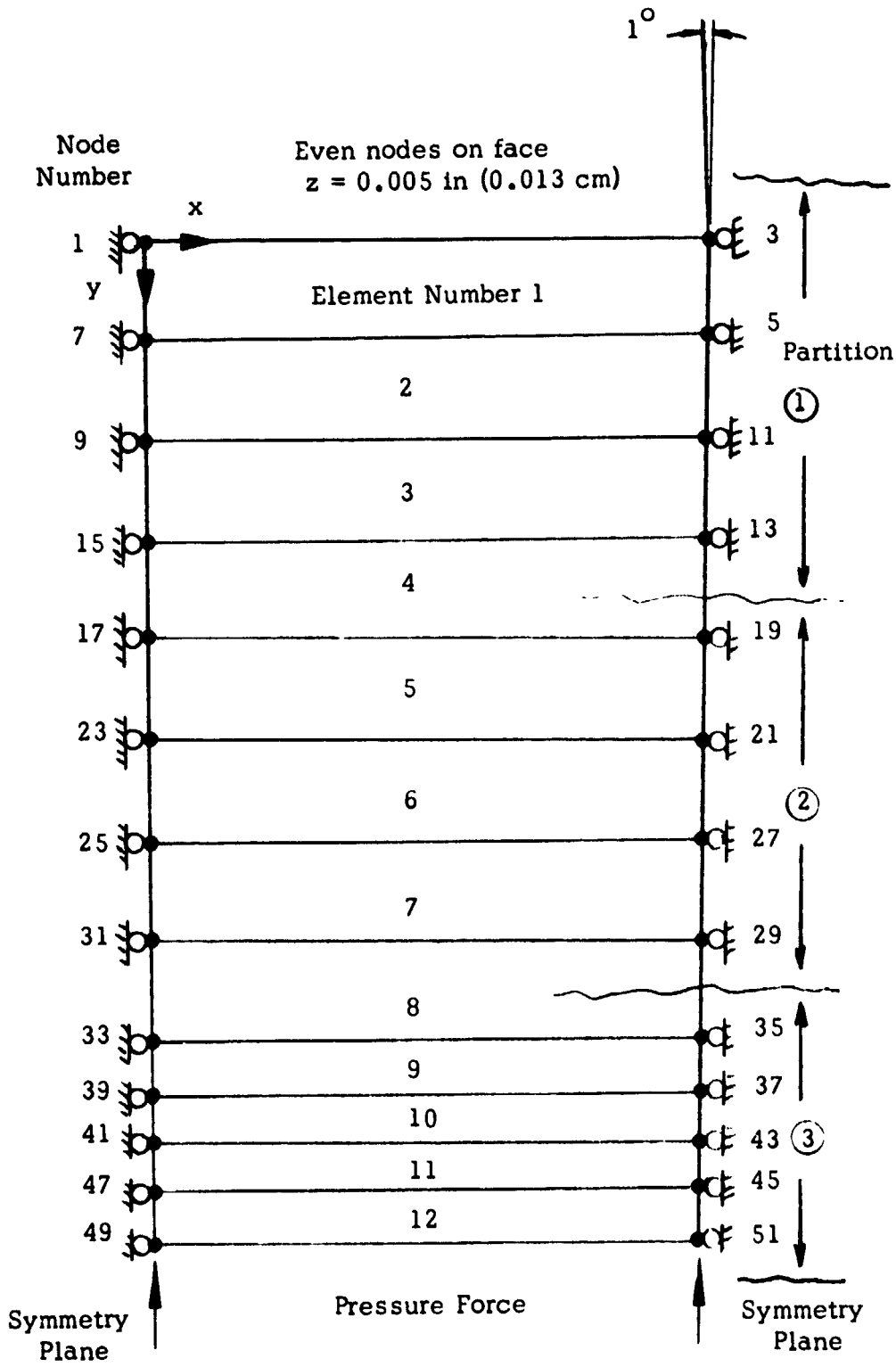

Figure 3. Finite element model.

The boundary conditions in the z-direction require special consideration. A very thin section was taken at the throat, so that the rocket engine contour curvature can be neglected. That is, constant thickness elements are used. Under load, the section remains plane; and also, the total load on the section is equal to the engine thrust load. This corresponds to the generalized plane strain condition.

Under these conditions an approximation for the axial boundary condition is obtained from the generalized plane strain equation of elasticity, namely (Reference 7)

$$\epsilon_z = \frac{1}{E} \left[\sigma_z - \nu (\sigma_x + \sigma_y)\right] \qquad (1)$$

The stress in the x-direction is computed from the hoop pressure load. Stresses in the y-direction are negligible. The z-component of stress is determined by the thrust load. Thus, the nodal points along the face z = 0 (odd numbers) are fixed and the nodal points on the opposite face (even numbers) are given the prescribed displacement determined from Equation (1). Since the nodal point forces in the z-direction are printed output for RETSCP, a post run evaluation of the net z force is made. If the result differs substantially from the thrust force value; then the z-direction displacement is adjusted and an iteration is performed. The reference temperature is taken to be the mean temperature; thus, the axial strain computed using equation (1) need not be adjusted for thermal growth.

During the engine firing, the throat pressure load is 175 psi ($121 \times 10^4 N/m^2$). The mean wall temperature is $1000^{\circ}F$ ($538^{\circ}C$) and a linear temperature gradient is assumed. That is, the outer wall is at $910^{\circ}F$ ($488^{\circ}C$) and the inner wall at $1090^{\circ}F$ ($588^{\circ}C$) with constant gradient through the thickness.

The material properties which were used in the calculation are listed in Table III, Reference 2 and 3. Input and output data for the hot engine firing pulse are given in Appexdixes B and C. See Reference 4 for card content and data format.

The important point to be noted, from the output data in Appendix C, is that the entire structure behaves elastically. Thus, there will be no residual strain influence on the engine-off portion of the stress-strain cycle.

The hoop stress component distribution is plotted in Figure 4. The result is nearly linear and corresponds to a linear temperature gradient across a thin wall cylinder. The hot inner wall corresponding to the engine run pulse is in compression; whereas, the cooler outer wall is in tension. The stress result for this engine run pulse is non-symmetrical with respect to the mean radius due to the chamber pressure load. The structural behavior is dominated by the thermal loading.

TABLE III

HAYNES 188 MATERIAL PROPERTIES DATA

Property	English Units (RETSCP)	Metric Units
Thermal Expansion Coefficient:	8.4×10^{-6} in/in-^{o}F	15.1×10^{-6} m/m-^{o}C
Modulus of Elasticity:	27.6×10^{6} psi	19.0×10^{10} N/m^{2}
Poisson's Ratio:	0.30	0.30
Plastic Modulus Ratio:	0.10	0.10
Yield Stress * :		
Reference Yield (σ_o)	43,800 psi	3.02×10^{8} N/m^{2}
Yield Slope (λ_1)	5.0 psi/ ^{o}F	$6.2 \times 10^{+4}$ N/m^{2} -^{o}C

* $\sigma_Y = \sigma_o - \lambda_1 \theta_r$

Where: $\theta_r = T - T_r$

$T_r = 1000^{o}$F (538^{o}C)

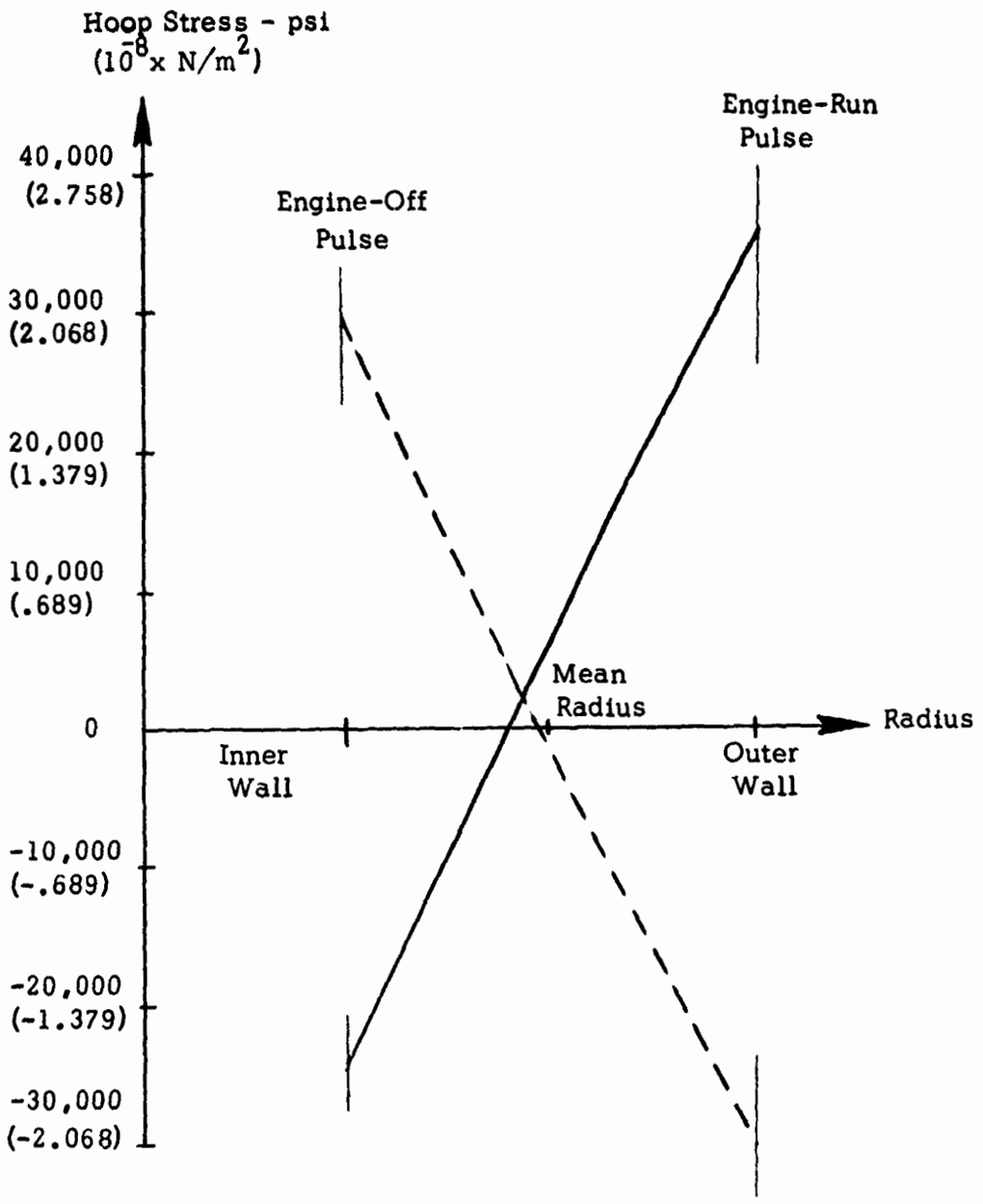

Figure 4. Hoop stress distribution.

The engine-off portion of the thruster pulse was computed in a manner analogous to that described above. That is, a linear temperature gradient between the opposite limits of 1090°F (588°C) on the outer wall and 910°F (488°C) on the inner wall. Also, the throat station chamber pressure is now zero and there is zero net thrust. The appropriate boundary condition, in the z-direction, is zero strain.

Results for the engine-off case are similar to the run condition; except that now the outer wall is in compression and the inner wall in tension. Again, the entire structure remains elastic. The hoop stress component distribution is plotted in Figure 4. Note, that in the absence of pressure loading, the stress distribution is nearly symmetrical with respect to the mean radius. The stress magnitudes are comparable for the engine-run and engine-off pulses. It should be noted that the outer wall stress and the inner wall stress alternates between tension and compression as the engine is cycled.

The effective, or total, strain is related to the effective stress via the material stress-strain data. Effective stress is defined as follows (Reference 4):

$$\sigma_e = \frac{1}{\sqrt{2}} \left[(\sigma_x-\sigma_y)^2 + (\sigma_x-\sigma_z)^2 + (\sigma_y-\sigma_z)^2 + 6\,(\tau_{xy}^2+\tau_{yz}^2+\tau_{xz}^2) \right]^{1/2} \qquad (2)$$

The distribution of effective strain is plotted in Figure 5 for both engine-run and engine-off pulses. Since the calculated effective stress can be positive or negative, it is necessary to consider the signs of the average x - and z - stress components to determine if the effective strain in Figure 5 is positive or negative (the y-stress is negligible when compared to the x - or z - stress components). The effective strain is considered positive when both the average x - and z - stress components are positive. Likewise, the effective stress is considered negative when both the average x - stress and z - stress components are negative. Near the zero strain axis, the x - and z - stress component signs differ so that the above criteria does not apply. In that case, smooth curves were drawn through the plotted points which met the sign criteria on either side of the axis. Associated with the tension-compression stress reversal, there is a corresponding strain reversal. Thus, a strain range is established for the engine pulse mode.

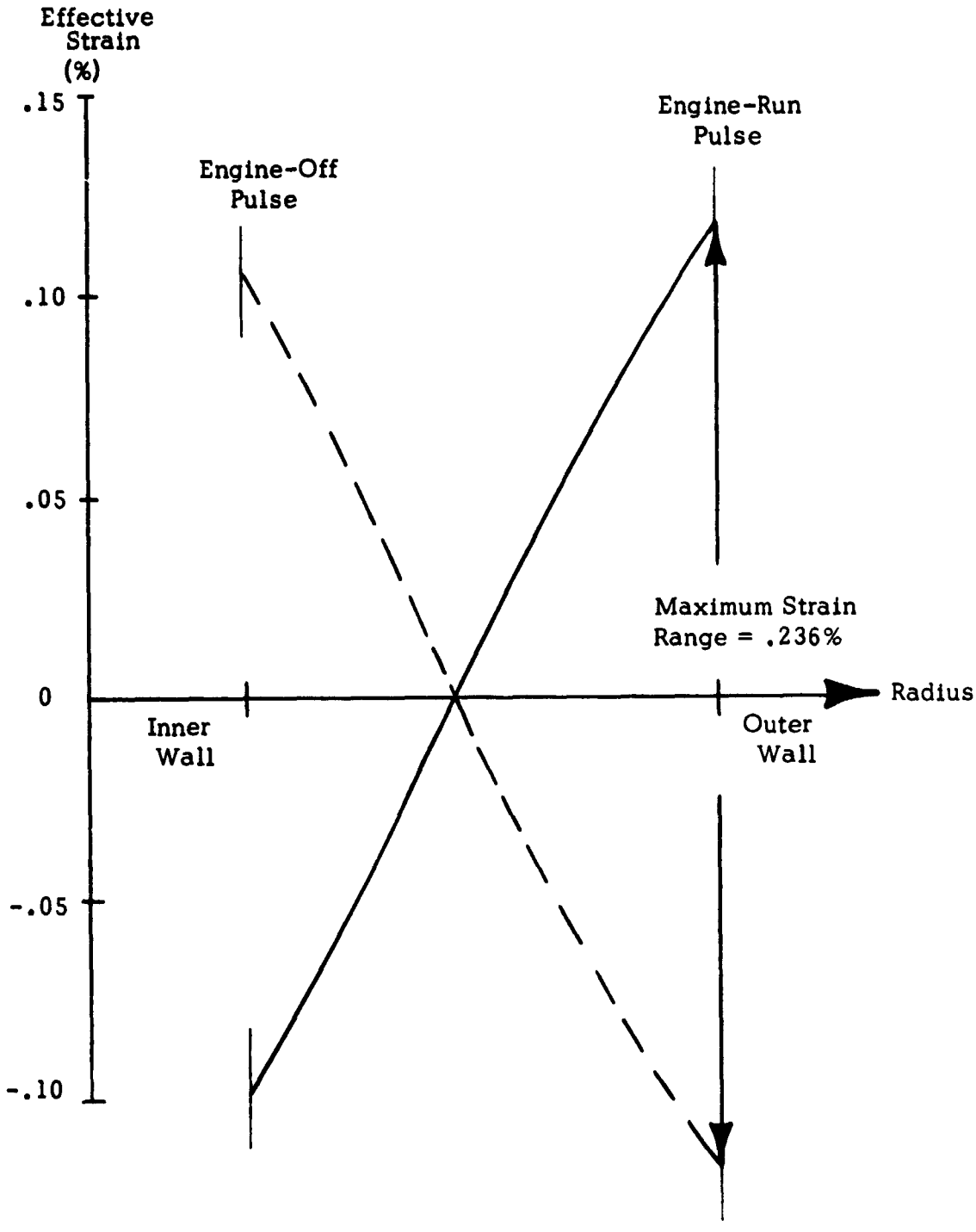

Figure 5. Effective strain distribution.

FATIGUE ANALYSIS

Prediction of chamber fatigue life is made by using the computed strain results in conjunction with uniaxial fatigue data.

In the case of Haynes 188, suitable fatigue test data are not available. Thus, strain-life curves are generated by the Universal Slopes method, Reference 6; namely,

$$\Delta \varepsilon_t = \frac{3.5\,\sigma_u}{E}\,\bar{N}_f^{\,-0.12} + \left[\ln \frac{1}{1-RA}\right]^{0.60} \bar{N}_f^{\,-0.60} \qquad (3)$$

where, the ultimate tensile strength σ_u, modulus of elasticity E, and reduction in area RA are based on the short term tensile test.

Now, for elevated test temperatures, the Universal Slopes prediction is modified, Reference 8. First, equation (3) is based on the short term properties at the elevated temperature. Then, to account for reduced life at elevated temperature, the "minimum" life N_f is defined as one tenth of the value in equation (3), $\bar{N}_f/10$. Average life is twice this minimum value. This procedure is based on a comparison with a great deal of experimental data.

Minimum life values were computed per the above method for temperatures in the range 700 - 1300°F (371-704° C). Results are presented in Figure 6. The curves coincide over the range considered. Typically at 1000°F (538°C), the fatigue life curve is based on $E = 27.6 \times 10^6$ psi (19.0×10^{10} N/m^2), σ_u = 107,200 psi (7.39×10^8 N/m^2), and RA = 0.60.

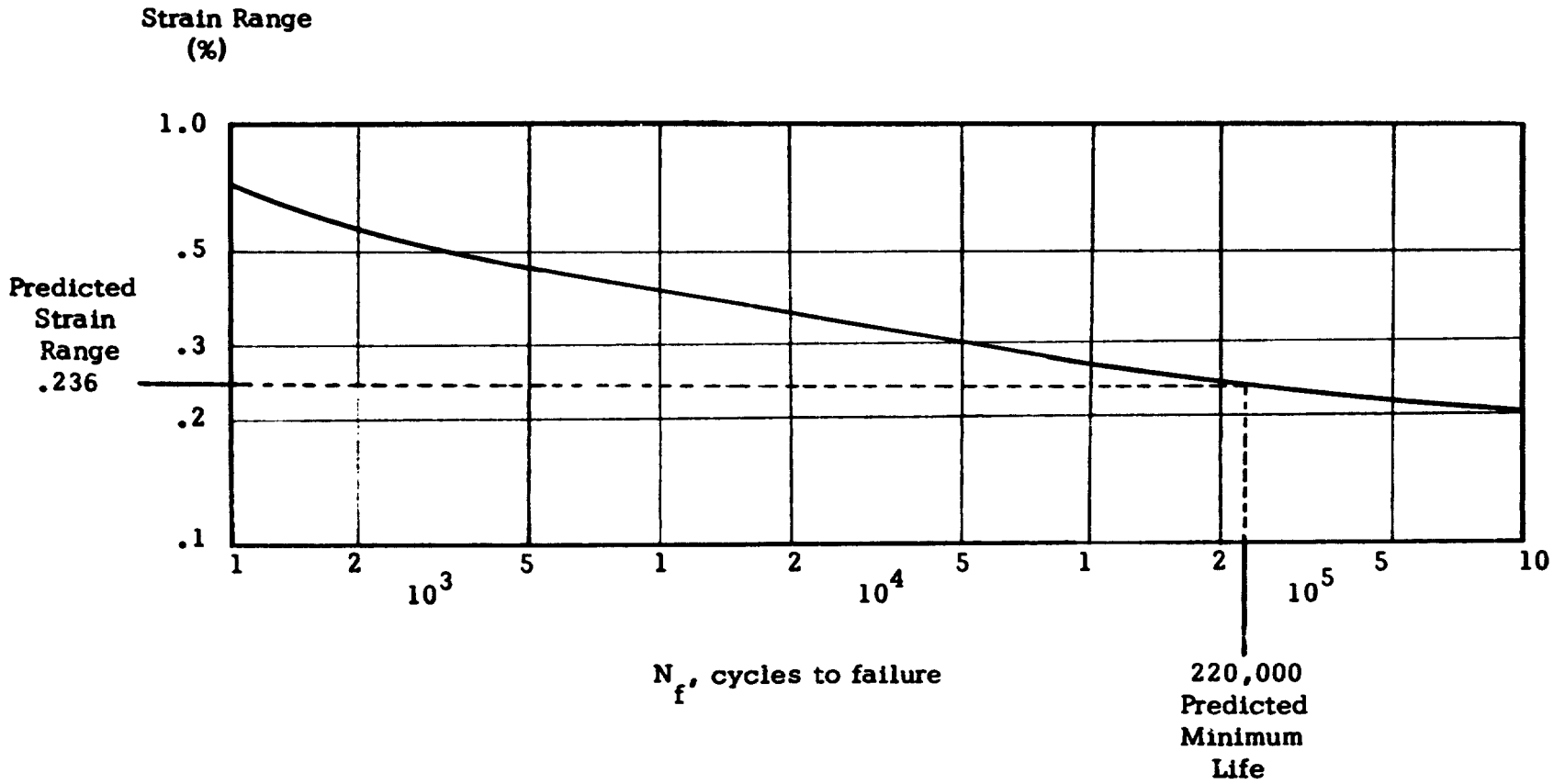

Figure 6. Minimum fatigue life for Haynes 188 at elevated temperature.

The linear cummulative damage law, Reference 9, is useful when the loading produces varying strain range values. According to that law, if n_j and n_k cycles are applied at conditions for which the fatigue life would be N_{f_j} and N_{f_k} respectively; then, the damage is accumulated linearly as follows:

$$D = \frac{n_j}{N_{f_j}} + \frac{n_k}{N_{f_k}} \tag{4}$$

Failure occurs when the cumulated damage totals unity.

For the case at hand, mean or typical loading conditions are assumed. Thus, the fatigue life is obtained directly from the material fatigue test data. Had the strain calculation been performed for various loading conditions; the life would be computed using equation (4). Much work has been done in the area of fatigue damage, along both the experimental and analytical lines. The topic is touched on briefly here only to indicate how an accurate loading spectrum would be treated.

Now, for the conditions at hand; fatigue life is determined directly by entering Figure 6 with the maximum value of strain range. The resulting predicted minimum life is 220,000 cycles. Recall that, the number of pulses, which the nozzle throat was subjected to without failure, was 50,825.

CONCLUDING REMARKS

The detailed life analysis presented herein was conducted for configuration and operating conditions which correspond directly to actual integrated thruster assembly test conditions. Thus, comparison of predicted and observed fatigue behavior is possible. The computed strain range was used to predict the minimum number of cycles to failure. The predicted minimum life was in fact greater than the number of pulses to which the thruster was subjected without failure.

The RETSP program has three-dimensional and elasto-plastic capability. Thus, the program and analytical procedure have potential for extended applications in attitude control thruster evaluation. For example, complex configurations of other locations within the engine could be analyzed in detail. These include the regeneratively cooled combustion chamber, and the film coolant exit lip.

Parametric studies, at the nozzle throat, could also be conducted. That is, the variation in fatigue life with chamber pressure, O/F ratio, and wall thickness could be determined. Also, by adding several rows of elements, the effects of axial temperature gradient and nozzle throat curvature could be studied.

Application of the above techniques would not only generate more efficient thruster designs; but would also increase understanding of the parameters which affect engine fatigue life.

APPENDIX A --- SYMBOLS

D	Fatigue damage fraction
E	Modulus of elasticity
n	Number of loading cycles
N_f	Minimum fatigue life
$\bar{N}_f$	Universal slopes cycles to failure
RA	Reduction in area
T	Temperature
T_r	Reference temperature
x,y,z	Cartesian coordinates
ϵ	Strain
θ	Temperature difference, $T - T_r$
σ	Stress
σ_e	Effective stress
$\sigma_x,\sigma_y,\sigma_z$	Normal stress components
σ_Y	Yield stress
σ_o	Yield stress at reference temperature
σ_U	Ultimate tensile strength
λ_1	Yield slope with temperature
τ	Shear stress
ν	Poisson's ratio

APPENDIX B --- SAMPLE RETSCP INPUT DATA

The following input listings are from the engine-run portion of the test cycle. The data are included as programming guidlines. For complete description of input data and format see Reference 4.

```
BEGIN EXECUTION.
 3  52  12  52   1   3   4   1   1   0   0
 1          0.              0.              0.
 2          0.              0.              0.0050
 3          0.0173          0.0002          0.
 4          0.0173          0.0002          0.0050
 5          0.0173          0.0031          0.
 6          0.0173          0.0031          0.0050
 7          0.              0.0030          0.
 8          0.              0.0030          0.0050
 9          0.              0.0060          0.
10          0.              0.0060          0.0050
11          0.0172          0.0061          0.
12          0.0172          0.0061          0.0050
13          0.0171          0.0091          0.
14          0.0171          0.0091          0.0050
15          0.              0.0090          0.
16          0.              0.0090          0.0050
17          0.              0.0120          0.
18          0.              0.0120          0.0050
19          0.0171          0.0121          0.
20          0.0171          0.0121          0.0050
21          0.0170          0.0151          0.
22          0.0170          0.0151          0.0050
23          0.              0.0150          0.
24          0.              0.0150          0.0050
25          0.              0.0180          0.
26          0.              0.0180          0.0050
27          0.0170          0.0181          0.
28          0.0170          0.0181          0.0050
29          0.0169          0.0211          0.
30          0.0169          0.0211          0.0050
31          0.              0.0210          0.
32          0.              0.0210          0.0050
33          0.              0.0240          0.
34          0.              0.0240          0.0050
35          0.0169          0.0241          0.
36          0.0169          0.0241          0.0050
37          0.0168          0.0256          0.
38          0.0168          0.0256          0.0050
39          0.              0.0255          0.
40          0.              0.0255          0.0050
41          0.              0.0270          0.
42          0.              0.0270          0.0050
43          0.0168          0.0271          0.
44          0.0168          0.0271          0.0050
45          0.0168          0.0286          0.
46          0.0168          0.0286          0.0050
47          0.              0.0285          0.
48          0.              0.0285          0.0050
49          0.              0.0300          0.
50          0.              0.0300          0.0050
51          0.0168          0.0301          0.
52          0.0168          0.0301          0.0050
 1   4   1  16
 4   8  17  32
 8  12  33  52
 1      438.0000          5.0000        100.0000          -0.
 1  27600000.0000          0.3000          8.4000
 2   4   6   8   1   3   5   7   1  -81.000
```

8	6	12	10	7	5	11	9	1	-63.000
10	12	14	16	9	11	13	15	1	-45.000
16	14	20	18	15	13	19	17	1	-27.000
18	20	22	24	17	19	21	23	1	-9.000
24	22	28	26	23	21	27	25	1	9.000
26	28	30	32	25	27	29	31	1	27.000
32	30	36	34	31	29	35	33	1	45.000
34	36	38	40	33	35	37	39	1	58.500
40	38	44	42	39	37	43	41	1	67.500
42	44	46	48	41	43	45	47	1	76.500
48	46	52	50	47	45	51	49	1	85.500

1	0	1	0	-0.	-0.	-0.	-0.
2	0	1	0	-0.	-0.	-0.	-0.
3	0	1	0	-0.	-0.	-0.	1.00000000
4	0	1	0	-0.	-0.	-0.	1.00000000
5	0	1	0	-0.	-0.	-0.	1.00000000
6	0	1	0	-0.	-0.	-0.	1.00000000
7	0	1	0	-0.	-0.	-0.	-0.
8	0	1	0	-0.	-0.	-0.	-0.
9	0	1	0	-0.	-0.	-0.	-0.
10	0	1	0	-0.	-0.	-0.	-0.
11	0	1	0	-0.	-0.	-0.	1.00000000
12	0	1	0	-0.	-0.	-0.	1.00000000
13	0	1	0	-0.	-0.	-0.	1.00000000
14	0	1	0	-0.	-0.	-0.	1.00000000
15	0	1	0	-0.	-0.	-0.	-0.
16	0	1	0	-0.	-0.	-0.	-0.
17	0	1	0	-0.	-0.	-0.	-0.
18	0	1	0	-0.	-0.	-0.	-0.
19	0	1	0	-0.	-0.	-0.	1.00000000
20	0	1	0	-0.	-0.	-0.	1.00000000
21	0	1	0	-0.	-0.	-0.	1.00000000
22	0	1	0	-0.	-0.	-0.	1.00000000
23	0	1	0	-0.	-0.	-0.	-0.
24	0	1	0	-0.	-0.	-0.	-0.
25	0	1	0	-0.	-0.	-0.	-0.
26	0	1	0	-0.	-0.	-0.	-0.
27	0	1	0	-0.	-0.	-0.	1.00000000
28	0	1	0	-0.	-0.	-0.	1.00000000
29	0	1	0	-0.	-0.	-0.	1.00000000
30	0	1	0	-0.	-0.	-0.	1.00000000
31	0	1	0	-0.	-0.	-0.	-0.
32	0	1	0	-0.	-0.	-0.	-0.
33	0	1	0	-0.	-0.	-0.	-0.
34	0	1	0	-0.	-0.	-0.	-0.
35	0	1	0	-0.	-0.	-0.	1.00000000
36	0	1	0	-0.	-0.	-0.	1.00000000
37	0	1	0	-0.	-0.	-0.	1.00000000
38	0	1	0	-0.	-0.	-0.	1.00000000
39	0	1	0	-0.	-0.	-0.	-0.
40	0	1	0	-0.	-0.	-0.	-0.
41	0	1	0	-0.	-0.	-0.	-0.
42	0	1	0	-0.	-0.	-0.	-0.
43	0	1	0	-0.	-0.	-0.	1.00000000
44	0	1	0	-0.	-0.	-0.	1.00000000
45	0	1	0	-0.	-0.	-0.	1.00000000
46	0	1	0	-0.	-0.	-0.	1.00000000
47	0	1	0	-0.	-0.	-0.	-0.
48	0	1	0	-0.	-0.	-0.	-0.
49	0	1	0	-0.	-0.	-0.	-0.

YOR4528 PRICE

50	0	1	0	-0.	-0.	-0.	-0.	
51	0	1	0	-0.	-0.	-0.	1.00000000	
52	0	1	0	-0.	-0.	-0.	1.00000000	

49	-0.	-0.0037	-0.
50	-0.	-0.0037	-0.
51	-0.	-0.0037	-0.
52	-0.	-0.0037	-0.

APPENDIX C --- SAMPLE RETSCP OUTPUT DATA

The following output data are from the engine-run portion of the test cycle. The nodal point displacements (inches), stress components (psi), and the yield check summary (inches/inch or psi where applicable) are included. For complete descirption of output data and formats see Reference 4.

NODE	X-DISPLACEMENTS	Y-DISPLACEMENTS	Z-DISPLACEMENTS
1	0.	-0.17882113E-03	-0.
2	-0.	-0.17882114E-03	-0.
3	0.31218773E-05	-0.17885229E-03	-0.
4	0.31218771E-05	-0.17885228E-03	-0.
5	0.31902520E-05	-0.18276948E-03	-0.
6	0.31902519E-05	-0.18276948E-03	-0.
7	-0.	-0.18282725E-03	-0.
8	-0.	-0.18282726E-03	-0.
9	-0.	-0.18602427E-03	-0.
10	-0.	-0.18602427E-03	-0.
11	0.32461363E-05	-0.18597110E-03	-0.
12	0.32461364E-05	-0.18597110E-03	-0.
13	0.32875067E-05	-0.18834120E-03	-0.
14	0.32875069E-05	-0.18834121E-03	-0.
15	-0.	-0.18838979E-03	-0.
16	-0.	-0.18838978E-03	-0.
17	0.	-0.18991922E-03	-0.
18	-0.	-0.18991921E-03	-0.
19	0.33143278E-05	-0.18987779E-03	-0.
20	0.33143278E-05	-0.18987779E-03	-0.
21	0.33265415E-05	-0.19057750E-03	-0.
22	0.33265413E-05	-0.19057749E-03	-0.
23	-0.	-0.19061123E-03	-0.
24	-0.	-0.19061122E-03	-0.
25	-0.	-0.19046314E-03	-0.
26	-0.	-0.19046309E-03	-0.
27	0.33241030E-05	-0.19043781E-03	-0.
28	0.33241024E-05	-0.19043777E-03	-0.
29	0.33069538E-05	-0.18945533E-03	-0.
30	0.33069521E-05	-0.18945523E-03	-0.
31	-0.	-0.18947309E-03	-0.
32	-0.	-0.18947288E-03	-0.
33	0.	-0.18763891E-03	-0.
34	-0.	-0.18763810E-03	-0.
35	0.32750521E-05	-0.18762768E-03	-0.
36	0.32750440E-05	-0.18762721E-03	-0.
37	0.32535320E-05	-0.18639479E-03	-0.
38	0.32535402E-05	-0.18639526E-03	-0.
39	-0.	-0.18640433E-03	-0.
40	-0.	-0.18640398E-03	-0.
41	-0.	-0.18495799E-03	-0.
42	-0.	-0.18495822E-03	-0.
43	0.32283224E-05	-0.18495053E-03	-0.
44	0.32283183E-05	-0.18495030E-03	-0.
45	0.31993987E-05	-0.18329350E-03	-0.
46	0.31994170E-05	-0.18329455E-03	-0.
47	-0.	-0.18330000E-03	-0.
48	-0.	-0.18330046E-03	-0.
49	-0.	-0.18142909E-03	-0.
50	-0.	-0.18143014E-03	-0.
51	0.31667387E-05	-0.18142241E-03	-0.
52	0.31667407E-05	-0.18142252E-03	-0.

ELEMENT NUMBER	FACE NODE NUMBERS			X,Y AND Z COORDINATES		
X-STRESS	Y-STRESS	Z-STRESS	XY-STRESS	YZ-STRESS	XZ-STRESS	
1	2 4 6 8		0.008650	0.001575	0.005000	
0.000863	-0.000663	0.000680	0.000024	-0.000000	-0.000000	
32337.713135	-45.885742	28466.594482	255.501459	-0.001970	-0.000244	
1	1 3 5 7		0.008650	0.001575	0.	
0.000863	-0.000663	0.000680	0.000024	-0.000000	-0.000000	
32337.725098	-45.847534	28466.596191	255.491058	-0.001815	-0.000166	
1	2 4 1 3		0.008650	0.000100	0.002500	
0.000861	-0.000662	0.000680	0.000020	-0.000000	-0.000000	
32278.322266	-45.499023	28448.886475	212.757458	-0.001970	-0.000198	
1	7 6 8 5		0.008650	0.003050	0.002500	
0.000865	-0.000663	0.000680	0.000028	-0.000000	-0.000000	
32397.115967	-46.233765	28484.304443	298.235023	-0.001834	-0.000190	
1	1 2 7 8		0.	0.001500	0.002500	
0.000866	-0.000655	0.000680	0.000024	-0.000000	-0.000000	
32585.337891	293.456787	28642.678223	251.166172	-0.019232	-0.000464	
1	6 4 5 3		0.017300	0.001650	0.002500	
0.000859	-0.000670	0.000680	0.000024	0.000000	0.000000	
32090.100830	-385.189331	28290.512939	259.826374	0.015505	0.000055	
AVERAGE STRESS FOR ELEMENT 1						
32337.718750	-45.866577	28466.595215	255.496218	-0.001892	-0.000224	
2	8 6 12 10		0.008625	0.004550	0.005000	
0.000716	-0.000537	0.000529	0.000022	-0.000000	-0.000000	
26469.203369	-122.825195	22509.834717	231.582272	-0.006874	-0.000022	
2	7 5 11 9		0.008625	0.004550	0.	
0.000716	-0.000537	0.000529	0.000022	-0.000000	-0.000000	
26469.206299	-122.816528	22509.835449	231.579277	-0.006816	-0.000059	
2	8 6 7 5		0.008650	0.003050	0.002500	
0.000714	-0.000533	0.000529	0.000022	-0.000000	-0.000000	
26449.219238	-16.633911	22535.695557	230.793962	-0.006932	-0.000149	
2	9 12 10 11		0.008600	0.006050	0.002500	
0.000718	-0.000541	0.000529	0.000022	-0.000000	0.000000	
26489.189453	-229.009277	22483.973633	232.367920	-0.006855	0.000004	
2	7 8 9 10		0.	0.004500	0.002500	
0.000716	-0.000537	0.000529	-0.000036	-0.000000	-0.000000	
26483.241211	-121.081055	22514.567871	-379.056664	-0.011701	-0.000257	
2	12 6 11 5		0.017250	0.004600	0.002500	
0.000715	-0.000537	0.000529	0.000079	-0.000000	0.000000	
26455.167969	-124.561523	22505.101807	842.218369	-0.001955	0.000118	
AVERAGE STRESS FOR ELEMENT 2						
26469.204590	-122.821533	22509.834717	231.580914	-0.006797	-0.000002	
3	10 12 14 16		0.008575	0.007550	0.005000	
0.000568	-0.000411	0.000378	0.000018	-0.000000	0.000000	
20594.290283	-199.105225	16551.344238	187.193806	-0.002250	0.000075	
3	9 11 13 15		0.008575	0.007550	0.	
0.000568	-0.000411	0.000378	0.000018	-0.000000	0.000000	
20594.273682	-199.160339	16551.344971	187.200623	-0.002114	0.000038	
3	10 12 9 11		0.008600	0.006050	0.002500	
0.000567	-0.000408	0.000378	0.000018	-0.000000	-0.000000	
20573.726318	-122.517700	16568.162354	186.531599	-0.002394	-0.000156	
3	15 14 16 13		0.008550	0.009050	0.002500	
0.000570	-0.000414	0.000378	0.000018	-0.000000	0.000000	

```
20614.837402    -275.747986    16534.526611     187.862745      -0.001979       0.000164
   3               9   10   15   16            0.              0.007500        0.002500
    0.000569       -0.000411        0.000378      -0.000024       0.000000      -0.000000
20604.704102    -191.060608    16556.892822    -250.943048       0.009462      -0.000145
   3              14   12   13   11            0.017150        0.007600        0.002500
    0.000568       -0.000411        0.000378       0.000059      -0.000000       0.000000
20583.859863    -207.205139    16545.796143     625.337486      -0.013821       0.000238

AVERAGE STRESS FOR ELEMENT  3
20594.281982    -199.132813    16551.344727     187.197155      -0.002211       0.000037

   4              16   14   20   18            0.008550        0.010550        0.005000
    0.000420       -0.000284        0.000227       0.000010       0.000000       0.000000
14683.562744    -263.113342    10585.807373     107.108438       0.007521       0.000037
   4              15   13   19   17            0.008550        0.010550        0.
    0.000420       -0.000284        0.000227       0.000010       0.000000       0.000000
14683.551636    -263.150391    10585.807617     107.118066       0.007637       0.000095
   4              16   14   15   13            0.008550        0.009050        0.002500
    0.000419       -0.000284        0.000227       0.000010       0.000000       0.000000
14659.810547    -263.133148    10578.683105     106.974545       0.007482       0.000007
   4              17   20   18   19            0.008550        0.012050        0.002500
    0.000421       -0.000285        0.000227       0.000010       0.000000      -0.000000
14707.303589    -263.130798    10592.931763     107.252157       0.007675      -0.000145
   4              15   16   17   18            0.              0.010500        0.002500
    0.000419       -0.000283        0.000227       0.000010       0.000000      -0.000000
14683.557129    -226.978577    10596.653442     107.113120       0.023055      -0.000130
   4              20   14   19   13            0.017100        0.010600        0.002500
    0.000420       -0.000285        0.000227       0.000010      -0.000000       0.000000
14683.557129    -299.285095    10574.961548     107.113396      -0.007927       0.000146

AVERAGE STRESS FOR ELEMENT  4
14683.557251    -263.132050    10585.807495     107.113311       0.007579       0.000037

   5              18   20   22   24            0.008525        0.013550        0.005000
    0.000270       -0.000156        0.000076       0.000009       0.000000      -0.000000
 8758.728149    -298.114777     4624.729675      93.910362       0.019222      -0.000160
   5              17   19   21   23            0.008525        0.013550        0.
    0.000270       -0.000156        0.000076       0.000009       0.000000      -0.000000
 8758.706421    -298.187927     4624.729797      93.915385       0.019256      -0.000160
   5              18   20   17   19            0.008550        0.012050        0.002500
    0.000269       -0.000155        0.000076       0.000009       0.000000      -0.000000
 8737.509766    -281.982498     4623.218201      93.513054       0.019179      -0.000174
   5              23   22   24   21            0.008500        0.015050        0.002500
    0.000271       -0.000157        0.000076       0.000009       0.000000      -0.000000
 8779.924438    -314.320221     4626.241272      94.312665       0.019314      -0.000154
   5              17   18   23   24            0.              0.013500        0.002500
    0.000270       -0.000155        0.000076       0.000000       0.000000      -0.000000
 8761.824219    -261.405365     4636.685669       1.394121       0.026946      -0.000028
   5              22   20   21   19            0.017050        0.013600        0.002500
    0.000271       -0.000157        0.000076       0.000018       0.000000      -0.000000
 8755.610107    -334.897430     4612.773804     186.431591       0.011554      -0.000370

AVERAGE STRESS FOR ELEMENT  5
 8758.717163    -298.151459     4624.729675      93.912840       0.019232      -0.000199

   6              24   22   28   26            0.008500        0.016550        0.005000
    0.000120       -0.000028       -0.000076       0.000001       0.000000      -0.000000
 2815.115845    -319.287155    -1337.872086      11.123850       0.059893      -0.000540
   6              23   21   27   25            0.008500        0.016550        0.
    0.000120       -0.000028       -0.000076       0.000001       0.000000      -0.000000
```

```
2815.022583    -319.599670    -1337.872375      11.131205       0.059869       -0.000482
  6              24   22   23   21            0.008500       0.015050       0.002500
   0.000120       -0.000028      -0.000076       0.000001       0.000000       -0.000000
2817.288422    -319.443222    -1337.206421      11.140720       0.059875       -0.000459
  6              25   28   26   27            0.008500       0.018050       0.002500
   0.000120       -0.000028      -0.000076       0.000001       0.000000       -0.000000
2812.849731    -319.443649    -1338.538162      11.114507       0.059895       -0.000620
  6              23   24   25   26            0.             0.016500       0.002500
   0.000119       -0.000026      -0.000076       0.000001       0.000000       -0.000000
2815.068878    -277.010361    -1325.142441      11.127788       0.069544       -0.000619
  6              28   22   27   21            0.017000       0.016600       0.002500
   0.000121       -0.000029      -0.000076       0.000001       0.000000       -0.000000
2815.069275    -361.876511    -1350.602142      11.127517       0.050224       -0.000500

AVERAGE STRESS FOR ELEMENT  6
2815.069214    -319.443344    -1337.872208      11.127595       0.059883       -0.000560

  7              26   28   30   32            0.008475       0.019550       0.005000
  -0.000031       0.000102       -0.000227      -0.000000       0.000000       -0.000000
-3148.828979    -324.241028    -7301.822266      -2.815641       0.212677       -0.001424
  7              25   27   29   31            0.008475       0.019550       0.
  -0.000031       0.000102       -0.000227      -0.000000       0.000000       -0.000000
-3149.168335    -325.378418    -7301.822571      -2.771361       0.212619       -0.001328
  7              26   28   25   27            0.008500       0.018050       0.002500
  -0.000031       0.000101       -0.000227      -0.000000       0.000000       -0.000000
-3170.484619    -370.013611    -7321.829407      -2.912057       0.212098       -0.001504
  7              31   30   32   29            0.008450       0.021050       0.002500
  -0.000031       0.000103       -0.000227      -0.000000       0.000000       -0.000000
-3127.512634    -279.605804    -7281.815430      -2.675125       0.213179       -0.001312
  7              25   26   31   32            0.             0.019500       0.002500
  -0.000032       0.000104       -0.000227       0.000024       0.000000        0.000000
-3153.288391    -275.433228    -7288.296387     251.782715       0.280052        0.001130
  7              30   28   29   27            0.016950       0.019600       0.002500
  -0.000030       0.000100       -0.000227      -0.000024       0.000000       -0.000000
-3144.708740    -374.186066    -7315.348328    -257.369854       0.145187       -0.003862

AVERAGE STRESS FOR ELEMENT  7
-3148.998566    -324.809509    -7301.822327      -2.793492       0.212639       -0.001385

  8              32   30   36   34            0.008450       0.022550       0.005000
  -0.000183       0.000232       -0.000378      -0.000008       0.000000       -0.000000
-9125.793091    -300.160034   -13261.537476     -85.836205       0.846229       -0.005365
  8              31   29   35   33            0.008450       0.022550       0.
  -0.000183       0.000232       -0.000378      -0.000008       0.000000       -0.000000
-9127.251831    -305.048279   -13261.538086     -85.669568       0.846103       -0.005269
  8              32   30   31   29            0.008450       0.021050       0.002500
  -0.000182       0.000232       -0.000378      -0.000008       0.000000       -0.000000
-9097.860718    -302.602661   -13252.938843     -85.583343       0.846036       -0.005032
  8              33   36   34   35            0.008450       0.024050       0.002500
  -0.000184       0.000233       -0.000378      -0.000008       0.000000       -0.000000
-9155.184448    -302.605530   -13270.136841     -85.922558       0.846354       -0.005658
  8              31   32   33   34            0.             0.022500       0.002500
  -0.000184       0.000233       -0.000378      -0.000008       0.000000       -0.000000
-9126.522949    -269.025818   -13251.464355     -85.752912       1.091553       -0.005195
  8              36   30   35   29            0.016900       0.022600       0.002500
  -0.000183       0.000231       -0.000378      -0.000008       0.000000       -0.000000
-9126.522995    -336.182373   -13271.611206     -85.752916       0.600741       -0.005536

AVERAGE STRESS FOR ELEMENT  8
-9126.522461    -302.604309   -13261.537842     -85.752953       0.846171       -0.005269
```

```
     9              34   36   38   40              0.008425      0.024800      0.005000
      -0.000298        0.000329      -0.000491      -0.000005      0.000000      -0.000000
  -13638.791748     -327.328674   -17749.715088     -52.729803      0.618601      -0.000141
     9              33   35   37   39              0.008425      0.024800      0.
      -0.000298        0.000330      -0.000491      -0.000005      0.000000      -0.000000
  -13634.544312     -313.172974   -17749.715576     -52.449703      0.618331      -0.000145
     9              34   36   33   35              0.008450      0.024050      0.002500
      -0.000298        0.000327      -0.000491      -0.000005      0.000000      -0.000000
  -13677.437012     -419.909790   -17791.843994     -52.675487      0.616603      -0.004368
     9              35   38   40   37              0.008400      0.025550      0.002500
      -0.000298        0.000332      -0.000491      -0.000005      0.000000      0.000000
  -13595.899048     -220.591980   -17707.586914     -52.503979      0.620330      0.004170
     9              33   34   39   40              0.            0.024750      0.002500
      -0.000301        0.000334      -0.000491       0.000100      0.000000      0.000000
  -13675.612915     -207.436340   -17727.554443    1063.158752      1.236295      0.000160
     9              38   36   37   35              0.016850      0.024850      0.002500
      -0.000295        0.000325      -0.000491      -0.000110      0.000000      -0.000000
  -13597.722900     -433.065369   -17771.876465    -1168.338135      0.000632      -0.000292

AVERAGE STRESS FOR ELEMENT  9
  -13636.667847     -320.250549   -17749.715332      -52.589691      0.618466      -0.000124

    10              40   38   44   42              0.008400      0.026300      0.005000
      -0.000374        0.000397      -0.000567      -0.000014      -0.000000      0.000000
  -16610.774902     -250.106567   -20707.693848     -144.875067      -0.060786      0.002130
    10              39   37   43   41              0.008400      0.026300      0.
      -0.000374        0.000397      -0.000567      -0.000014      -0.000000      0.000000
  -16611.133545     -251.286377   -20707.695801     -144.719103      -0.061152      0.002052
    10              40   38   39   37              0.008400      0.025550      0.002500
      -0.000373        0.000396      -0.000567      -0.000014      -0.000000      0.000000
  -16588.187256     -250.694824   -20700.864258     -144.661108      -0.060853      0.008185
    10              41   44   42   43              0.008400      0.027050      0.002500
      -0.000375        0.000397      -0.000567      -0.000014      -0.000000      -0.000000
  -16633.721680     -250.697998   -20714.525635     -144.932837      -0.061056      -0.004089
    10              39   40   41   42              0.            0.026250      0.002500
      -0.000374        0.000397      -0.000567      -0.000014      0.000000      0.000000
  -16610.956543     -236.117065   -20703.321777     -144.796926      0.124525      0.002038
    10              44   38   43   37              0.016800      0.026350      0.002500
      -0.000374        0.000396      -0.000567      -0.000014      -0.000000      0.000000
  -16610.952393     -265.276123   -20712.068115     -144.797098      -0.246458      0.002106

AVERAGE STRESS FOR ELEMENT 10
  -16610.954346     -250.696289   -20707.694824      -144.797091      -0.060969      0.002052

    11              42   44   46   48              0.008400      0.027800      0.005000
      -0.000451        0.000462      -0.000642      -0.000016      -0.000000      0.000000
  -19640.873779     -254.128296   -23701.278564     -167.684774      -0.802088      0.007476
    11              41   43   45   47              0.008400      0.027800      0.
      -0.000451        0.000462      -0.000643      -0.000016      -0.000000      0.000000
  -19636.296387     -238.832886   -23701.280273     -167.758469      -0.802522      0.007437
    11              42   44   41   43              0.008400      0.027050      0.002500
      -0.000450        0.000462      -0.000643      -0.000016      -0.000000      0.000000
  -19612.481201     -246.479126   -23693.447754     -167.566250      -0.802377      0.000293
    11              47   46   48   45              0.008400      0.028550      0.002500
      -0.000452        0.000463      -0.000643      -0.000016      -0.000000      0.000000
  -19664.688721     -246.481567   -23709.110840     -167.877254      -0.802204      0.014489
    11              41   42   47   48              0.            0.027750      0.002500
      -0.000451        0.000463      -0.000643      -0.000016      -0.000000      0.000000
  -19638.588135     -231.572388   -23696.807861     -167.721663      -0.740298      0.007456
```

```
      11                  46    44    45    43                0.016800       0.027850       0.002500
       -0.000451            0.000462          -0.000643          -0.000016          -0.000000          0.000000
   -19638.582031       -261.388916     -23705.750977       -167.721844          -0.864312          0.007514

 AVERAGE STRESS FOR ELEMENT 11
   -19638.584961       -246.480469     -23701.279297       -167.721752          -0.802300          0.007437

      12                  48    46    52    50                0.008400       0.029300       0.005000
       -0.000529            0.000529          -0.000718          -0.000018          -0.000000          0.000000
   -22651.047607       -190.675049     -26675.527832       -190.171007          -1.419791          0.010685
      12                  47    45    51    49                0.008400       0.029300       0.
       -0.000529            0.000529          -0.000718          -0.000018          -0.000000          0.000000
   -22652.128174       -194.214478     -26675.531250       -190.216629          -1.420178          0.010626
      12                  48    46    47    45                0.008400       0.028550       0.002500
       -0.000528            0.000529          -0.000718          -0.000018          -0.000000          0.000000
   -22622.106689       -192.442261     -26666.684326       -190.017969          -1.419502          0.010227
      12                  49    52    50    51                0.008400       0.030050       0.002500
       -0.000530            0.000530          -0.000718          -0.000018          -0.000000          0.000000
   -22681.068604       -192.445923     -26684.374023       -190.369596          -1.420429          0.010722
      12                  47    48    49    50                0.             0.029250       0.002500
       -0.000529            0.000529          -0.000718          -0.000018          -0.000000          0.000000
   -22651.591553       -201.921753     -26678.373535       -190.193800          -1.605392          0.010621
      12                  52    46    51    45                0.016800       0.029350       0.002500
       -0.000529            0.000529          -0.000718          -0.000018          -0.000000          0.000000
   -22651.583740       -182.967163     -26672.685059       -190.193611          -1.234577          0.010747

 AVERAGE STRESS FOR ELEMENT 12
   -22651.587402       -192.444336     -26675.529297       -190.193817          -1.419994          0.010607
```

YIELD CHECK AFTER 1 ITTERATIONS

ELEMENT	TOTAL STRAIN	PLASTIC STRAIN	EFFECTIVE STRESS	YIELD STRESS	SECANT MODULUS	SECANT POISSON
1	0.001110	0.	30635.2	44205.0	27600000.0	0.3000
2	0.000900	0.	24853.3	44115.0	27600000.0	0.3000
3	0.000692	0.	19098.4	44025.0	27600000.0	0.3000
4	0.000485	0.	13378.4	43935.0	27600000.0	0.3000
5	0.000285	0.	7855.1	43845.0	27600000.0	0.3000
6	0.000136	0.	3749.0	43755.0	27600000.0	0.3000
7	0.000220	0.	6078.7	43665.0	27600000.0	0.3000
8	0.000415	0.	11466.0	43575.0	27600000.0	0.3000
9	0.000572	0.	15780.5	43507.5	27600000.0	0.3000
10	0.000679	0.	18749.1	43462.5	27600000.0	0.3000
11	0.000787	0.	21712.4	43417.5	27600000.0	0.3000
12	0.000896	0.	24720.2	43372.5	27600000.0	0.3000

REFERENCES

1. LaBotz, R. J., and Blubaugh, A.L., Integrated Thruster Assembly Program, NASA CR-134509, 1973.

2. Herchenroedet, R. B., Matthews, S. J., Tackett, J.W., and Wlodek, S. T., Haynes Alloy No. 188, Cobalt, March, 1972.

3. Anon., Haynes Alloy No. 188, Cabot Corporation, Stellite Division, 1973.

4. Miller, R. W., RETSCP: A Computer Program for Analysis of Rocket Engine Thermal Strains with Cyclic Plasticity, NASA CR-134640, June, 1974.

5. Manson, S.S., Thermal Stress and Low-Cycle Fatigue, McGraw-Hill Book Company, 1966.

6. Manson, S.S., Fatigue, A Complex Subject - Some Simple Approximations, Experimental Mechanics, July, 1965.

7. Wang, C., Applied Elasticity, McGraw-Hill Book Company, New York, 1953.

8. Manson, S.S., and Halford, G., A Method of Estimating High Temperature Low Cycle Fatigue Behavior of Materials, NASA TM-X-52270, 1967.

9. Langer, B.F., Fatigue Failure from Stress Cycles of Varying Amplitude, Journal of Applied Mechanics, 1937.